RSC Advances

This is an *Accepted Manuscript*, which has been through the Royal Society of Chemistry peer review process and has been accepted for publication.

Accepted Manuscripts are published online shortly after acceptance, before technical editing, formatting and proof reading. Using this free service, authors can make their results available to the community, in citable form, before we publish the edited article. This *Accepted Manuscript* will be replaced by the edited, formatted and paginated article as soon as this is available.

You can find more information about *Accepted Manuscripts* in the **Information for Authors**.

Modified hierarchical TiO$_2$ NTs for enhanced gas phase photocatalytic activity

Di Gu, Hongjun Wu[*], Yanji Zhu and Baohui Wang

Provincial Key Laboratory of Oil&Gas Chemical Technology, College of Chemistry & Chemical Engineering, Northeast Petroleum University, Daqing 163318, China.
E-mail: hjwu@nepu.edu.cn

In this paper, three kinds of noble metal nanoparticles (NMNs) were successfully loaded on hierarchical TiO$_2$ nanotube arrays (TiO$_2$ NTs) to improve photocatalytic (PC) activity of gas phase pollutants. The hierarchical TiO$_2$ NTs, with unique top-nanoporous and bottom-nanotubular structure, were prepared through a facile two-step anodization method, and then the noble metal nanoparticles were loaded on the TiO$_2$ NTs by means of a photo-reduction method. The gas phase photocatalytic activity of TiO$_2$ NTs and NMNs/TiO$_2$ NTs were estimated by decomposition of gaseous methanol. The formation of Schottky junctions between TiO$_2$ NTs and NMNs significantly improved the PC due to they could significantly accelerate the electron transfer and thus reduction of the recombination of photogenerated electrons and holes.

Introduction

Photocatalytic (PC) technology has received widespread attention for pollutants decomposition, and a lot of materials, especially metal oxide semiconductors, have been widely utilized as photocatalysts.[1-3] Among them, titanium dioxide (TiO$_2$) is regarded as one of the most promising photocatalysts because of its unique electronic properties, high resistance to photo-corrosion and low cost.[4-6] TiO$_2$ nanotube arrays (TiO$_2$ NTs), fabricated by electrochemical anodization process, have been demonstrated to be one of the most efficient materials of PC applications for degradation of environmental pollutants and conversion of solar energy because of their unique monodirectional electron transfer, high electron mobility and one-dimensional nanostructure.[7-9] In this paper, we fabricated a unique hierarchical TiO$_2$ combined nanostructure of top-nanorings and bottom-nanotubes by a two-step anodization method, which showed better PC activity than pure TiO$_2$ NTs due to its higher hierarchical and light scattering activity.[10]

However, unmodified TiO$_2$ as a wide bandgap semiconductor is limited to PC activity only under UV irradiation. For further enhancing PC activity of TiO$_2$ NTs and harvesting long wavelength radiation, noble metal nanoparticles (NMNs) modification were an effective option. Previous researches[11-16] have shown that the deposition of noble metals in the surface of TiO$_2$ nanoparticles can improve the photocatalytic activity of TiO$_2$ significantly. In this paper, three kinds of NMNs (Ag, Au, Pt) were investigated to select one would be best favorable for formation a Schottky junction with TiO$_2$ (Scheme 1). As the electron affinity of anatase TiO$_2$ is significantly lower than the work function of noble metal, which will induce higher electronic potential between noble metal and TiO$_2$, accelerating the electron transfer and

inhibits the electron-hole pairs recombination. The significance of this work provide a fundamental understanding not only to the fabrication but also the utility of Schottky junctions for enhanced environmental remediation method.
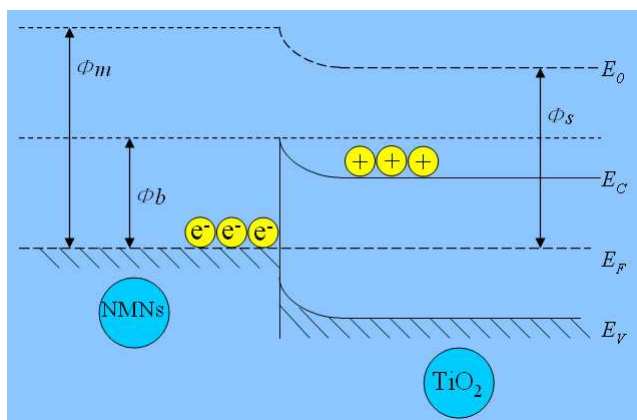
Scheme 1. Schematic Illustration of the Energy Bands between NMNs and TiO_2 NTs

Even the PC studies on TiO_2 with/without NMNs have been extensively studied, however, previous studies were focused on PC activity in aqueous solution,[17-20] the PC activity in gas phase has rarely studied. Compared with liquid phase reaction process, gas phase photocatalytic oxidation reaction features high reaction velocity, good exploitation rate of light, large volume flow, which could oxidize reactant completely and free of solvent influence,[21-24] and therefore lead to the wide application. To the best of our knowledge, the gas phase PC activity of NMNs decorated hierarchical TiO_2 NTs has not been reported. In this study, the gas phase PC activity of TiO_2 NTs and NMNs/TiO_2 NTs were estimated by decomposition of evaporated methanol.

Experimental

Chemicals and materials

Titanium foil (0.2mm thick, 99.6%, Strem Chemicals) was cut into pieces of 25×10 mm^2. Silver nitrate (I) ($AgNO_3$, Sigma-Aldrich Chemicals, 99%) was used as the precursor of Ag nanoparticles. Gold (III) acid chloride trihydrate ($HAuCl_4 \cdot 4H_2O$, Sigma-Aldrich Chemicals, 99%) was used as the precursor of Au nanoparticles. Platinum (II) acetylacetonate ($Pt(AcAc)_2$, Sigma-Aldrich Chemicals, 99%) was used as the precursor of Pt nanoparticles. Ethylene glycol (EG), ammonia fluoride (NH_4F) and methanol were purchased from Acros Organics and used as received.
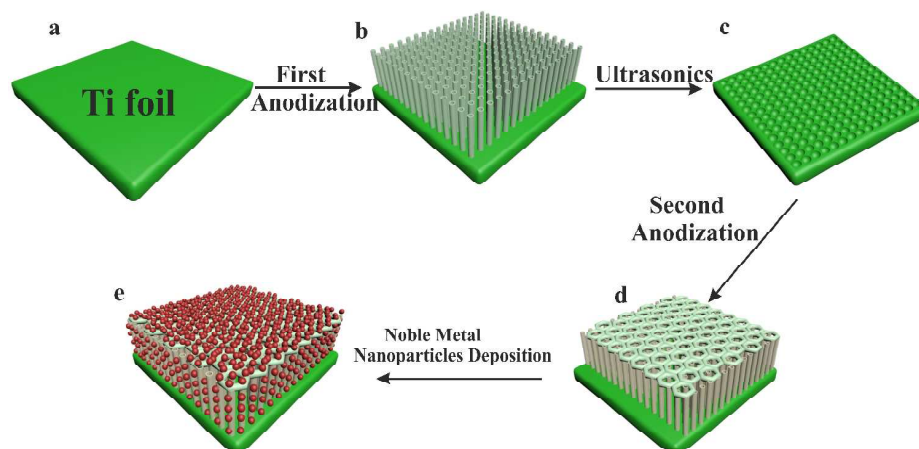
Scheme 2. Two-step anodization processes for fabrication of hierarchical TiO$_2$ NTs and photocatalytic reduction for decoration of NMNs.

Preparation of hierarchical TiO$_2$ NTs

The hierarchical TiO$_2$ NTs were fabricated by a two-step anodization process (Scheme 2a-d). Prior to anodization, the Ti foils were frist ultrasonically cleaned with ethanol and room-temperature distilled water, followed by drying in N$_2$ gas. The anodization was carried out using a conventional two-electrode system with the Ti foil as an anode and a Pt gauze (Aldrich, 100 mesh) as a cathode respectively. All electrolytes consisted of 0.5 wt% NH$_4$F in EG solution with 2 vol% water. All the anodization experiments were carried out at room temperature. In the first-step anodization, the Ti foil was anodized at 50 V for 30 min, then the as-grown nanotube layer was ultrasonically removed in deionized water, leaving compact two-dimensional hexagonal pattern on the surface of the Ti foil alone. The patterned Ti foil then underwent the second anodization at 20 V for 30 min, in which the hexagonal pattern formed top-porous structure and subjective NTs grew below the top-porous layer.[25] After second-step anodization, the prepared TiO$_2$ NTs sample was cleaned with distilled water and dried off with N$_2$ gas. The as-anodized TiO$_2$ NTs were annealed in air at 450 °C for 1 h with a heating rate of 5 °C/min.

Decoration of NMNs on TiO$_2$ NTs

Photocatalytic reduction method[26] was used to deposit NMNs on the TiO$_2$ NTs using AgNO$_3$, HAuCl$_4$, Pt(AcAc)$_2$ as precursor (Scheme 2e). The AgNO$_3$ aqueous solution was 1.0×10^{-2} mol/L (Fig. S1, ESI†), the HAuCl$_4$ aqueous solution was 2.43×10^{-4} mol/L (Fig. S2†), the Pt(AcAc)$_2$[27] was diluted in deionized water and ethanol with a water/ethanol volume ratio of 10:1, and the concentration of Pt(AcAc)$_2$ was fixed at 1.0×10^{-3} mol/L (Fig. S3 †). The Ti foil containing the prepared TiO$_2$ NTs were soaked into the precursor solution for 24h and then was irradiated in this solution with a

300 W high pressure mercury lamp for 30min to reduce the absorbed Ag^+ to Ag^0, Au^{3+} to Au^0 and Pt^{2+} to Pt^0 by photocatalysis at the expense of water oxidation.

Characterization of NMNs/TiO$_2$ NTs

The morphology of nanotubular structures and distribution of nanoparticles were determined by filed-emission scanning electron microscope (FESEM, Zeiss SigmaHV) and transmission electron microscope (TEM, Tecnai T12). The chemical compositions of NMNs/TiO$_2$ NTs were analyzed by energy dispersive spectrometer (EDS) equipped with FESEM. The crystal structures were characterized by grazing incidence X-ray diffraction (GIXRD) analysis by an X-ray diffractometer (Rigaku D/MAX-2200) with Cu Kα source in the range of 2ϑ = 20-70°. UV-visible diffuse reflectance spectra was obtained on a UV-visible spectrophotometer (Lambda 750) equipped with an integrating sphere assembly. Fine BaSO$_4$ powders were used as flectance standard.

The photoelectrochemical measurements were carried out in a three-electrode cell in 0.5 M Na$_2$SO$_4$ as the aqueous electrolyte with a electrochemical analyzer (WaveNow, PINE). TiO$_2$ NTs and NMNs/TiO$_2$ NTs were used as working electrodes, Ag/AgCl was used as the reference electrode and Pt foil was used as the counter electrode. The photoresponse was evaluated under chopped light irradiation (light on/off cycles: 60 s) at a fixed electrode potential of 0.5 V. The photocurrent was measured under irradiation from a 300 W high pressure mercury lamp. All measurements were carried out under ambient conditions at room temperature.

Gas phase PC degradation experiments

The gas phase PC activities of TiO$_2$ NTs and NMNs/TiO$_2$ NTs were detected by decomposition of evaluated methanol (5 μL). The decomposition rate of methanol was calculated through Fourier transform infrared (FTIR) spectroscopy (Bruker Tensor27). All the PC measurements were performed in a homemade cylindrical cell with 5 cm length and 3.6 cm width (Fig. S4 †), in which the TiO$_2$ NTs and NMNs/TiO$_2$ NTs samples were contained respectively. PC degradation of methanol was carried out with the irradiation of a 300 W high pressure mercury lamp (XC140408, Shanghai YaMing Lighting Co., Ltd.).

Results and discussion
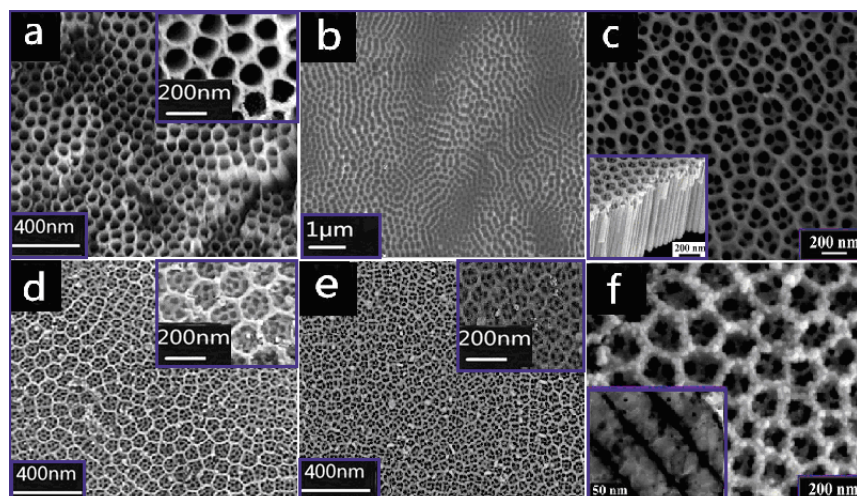
Fig. 1. Morphology of TiO$_2$ NTs: (a) TiO$_2$ NTs in the one-step anodization; (b)The Ti surface after the removal of one-step TiO$_2$ NTs layer; (c) hierarchical TiO$_2$ NTs in the second anodiztion step; hierarchical Ag/TiO$_2$ NTs (d) , Au/TiO$_2$ NTs(e) and Pt/TiO$_2$ NTs (f), the inset of (f) shows the TEM image of Pt nanoparticles inside the TiO$_2$ NTs.

Fig. 1a shows the SEM image of TiO$_2$ NTs in the frist step anodization, It can be seen from the figure that the structure of TiO$_2$ NTs is very loose. Fig. 1b shows the compact two-dimensional hexagonal pattern left on the Ti foil after the one-step TiO$_2$ NTs were removed by ultrasonic treatment in deionized water. Fig. 1c shows a top view SEM image of hierarchical TiO$_2$ NTs in the second step. Individual top hexagonally porous structure is fairly observed, with an average diameter of ~150 nm and a wall-thickness of ~20 nm (Fig. S5†). A cross-sectional view of the TiO$_2$ NTs is presented in the bottom-left inset of Fig. 1c, indicates corresponding tubular structure with a length of 1μm. It can be seen from Fig. 1d and Fig. 1e that Ag and Au nanoparticles are decorated on the surface of TiO$_2$ NTs. Fig. 1f is a high-magnification top-view SEM image of Pt/TiO$_2$ NTs. The TEM image of Pt/TiO$_2$ NTs is presented in the inset of Fig. 1f, which clearly showed Pt nanoparticles are not only decorated on the outer side of NT but also into the inter side of NTs with same diameter size of ~ 20nm as shown in SEM image.
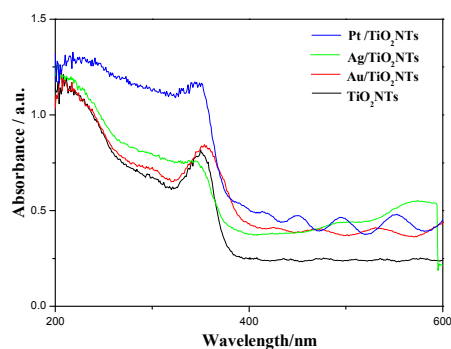
Fig. 2. Diffuse reflectance UV-vis absorption spectra of the NMNs/TiO$_2$ NTs.
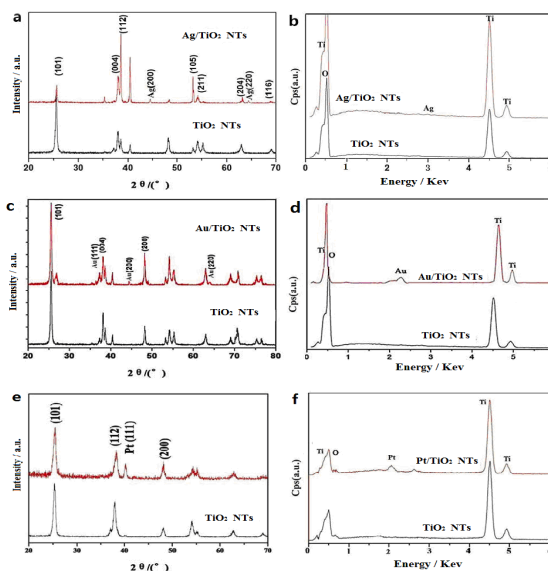
Fig. 3. XRD patterns and EDS spectra of TiO$_2$ NTs and NMNs/TiO$_2$ NTs: (a)(b)TiO$_2$ NTs and Ag/TiO$_2$ NTs; (c)(d)TiO$_2$ NTs and Au/TiO$_2$ NTs; (e)(f)TiO$_2$ NTs and Pt/TiO$_2$ NTs;

Optical absorption and crystalline are two important parameters for PC performance on TiO$_2$ materials. Materials with better optical absorption and higher crystallinity will subsequently result in a better PC performance. Therefore, UV-vis absorption spectra and XRD measurement were employed to characterize the optical absorption properties and crystallinity of NMNs/TiO$_2$ NTs (Fig.2 and Fig.3). As shown in Fig.2, all modified TiO$_2$ NTs samples depicted better UV absorption than unmodified TiO$_2$ NTs samples, as the Schottky junctions facilitate the electron transfer and thus reduce the recombination of electrons and holes, both contributing to enhanced PC performance. The XRD patterns of the hierarchical TiO$_2$ NTs and NMNs/TiO$_2$ are shown in Fig. 3. Clearly, both of them presented pure crystalline anatase with strong preferential orientation of (101). In addition, the NMNs/TiO$_2$ sample shows an extra noble metal XRD pattern with strong orientation of (111), which implies that the noble metal nanoparticles are successfully doped on the TiO$_2$ NTs. The EDS spectra in Fig. 3 showed another evidence for noble metal existence on the TiO$_2$ NTs.
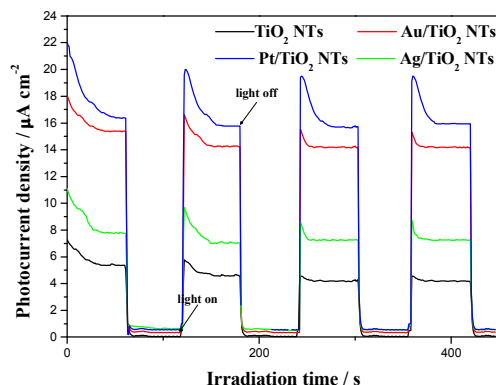
Fig. 4. Amperometric I−t curves at an applied potential of 0.5V under illumination of 300 W high pressure mercury lamp with 60 s light on/off cycles.

The photoresponse of the TiO_2 NTs electrode and NMNs/TiO_2 NTs electrode were investigated under illumination of 300 W high pressure mercury lamp with a bias of 0.5 V (vs Ag/AgCl). It can been seen from Fig. 4, all modified TiO_2 NTs samples depicted better reproducibility and stability as the light was turned on and off. The photocurrent decreased almost to zero instantly as soon as the illumination was interrupted and the photocurrent came back close to the original value as the illumination was turned on. It is interesting to note that the Pt/TiO_2 NTs composite electrode exhibited a photocurrent density of ~20 μA cm^{-2}, which was about 4 times larger than that of the unmodified TiO_2 NTs electrode with a photocurrent density of ~5μA cm^{-2}. The remarkably enhanced photocurrent may be ascribed to the formed Schottky junctions between TiO_2 NTs and NMNs in which have a fast electron transport and a more efficient separation of the photogenerated holes and electrons.
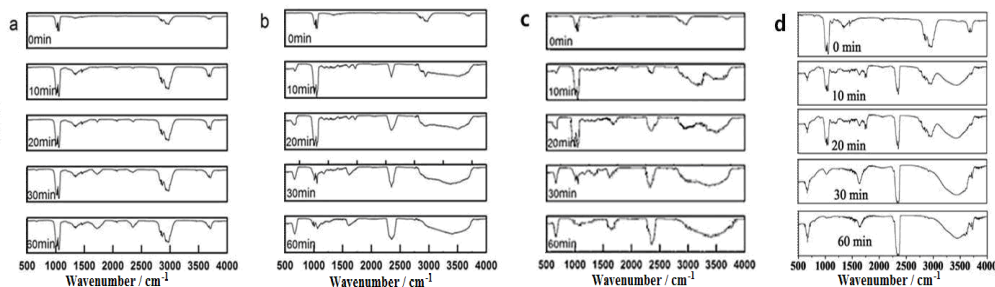
Fig. 5. Decomposition of methanol on TiO_2 NTs (a), Ag/ TiO_2 NTs (b), Au/ TiO_2 NTs (c) and Pt/ TiO_2 NTs (d) respectively as a function of irradiation time.

The photocatalytic activity of NMNs/TiO_2 NTs are evaluated by decomposition of methanol. Fig. 5 shows the FTIR spectra of methanol decomposition as a function of irradiation time on TiO_2 NTs, Ag/TiO_2 NTs, Au/TiO_2 NTs and Pt/TiO_2 NTs respectively.

Before the illumination, the initial methanol processes the bands at 1031, 1055, 1340, 2860, 2950, and 3685 cm^{-1}, Which bands correspond to the C-O stretching, CH_3 rocking, O-H bending, C-H parallel symmetric stretching, C-H out of plane asymmetric stretching, O-H stretching, respectively.[28-31] As the increase of irradiation time, all these bands started to decrease in intensity and new peaks appeared at 669, 1456, 1640, 1750, 2360 and 3440cm^{-1}. The band at 1456cm^{-1} can be assigned to the out of plane asymmetric bending of C-H, 1640 cm^{-1} proved the formation of isolated C=C bonds, and 1750cm^{-1} can be assigned to the C=O stretching vibration modes.[32-33] The gaseous CO_2 is a linear molecule with two infrared active absorption bands at 2360cm^{-1} (antisymmetric stretching mode) and 669cm^{-1} (bending mode).[34-35] Hence, one can conclude that the primary two peaks centered at 2360cm^{-1} and 669cm^{-1} imply the formation of CO_2 gas when methanol is decomposed. In the end, after 60 min, just CO_2 and H_2O existence as the results of completed decomposition of methanol on the Pt/TiO_2 NTs sample.

Based on the photocatalytic experimental data, we summarized the CO_2 transmittance peak height (2360 cm^{-1}, CO_2) for TiO_2 NTs, Ag/TiO_2 NTs, Au/TiO_2 NTs and Pt/TiO_2 NTs respectively in Fig. 6a. The experimental data of Fig. 6a were found to fit approximately a pseudo-first-order kinetic model by the linear transforms $f(t)= f_{inf}[1 - exp(-kt)]$ (f is peak height, f_{inf} is peak height at infinite time, and k is rate constant).[36] The corresponding curves were presented in Fig. 6b, and the values of rate constant $k_{TiO2\ NTs}= 0.0142 < k_{Ag/TiO2\ NTs} = 0.0731 < k_{Au/TiO2\ NTs} = 0.1031 < k_{Pt/TiO2\ NTs} = 0.1558$. Clearly, the Pt/$TiO_2$ NTs showed higher k value than hierarchical TiO_2 NTs and other noble metal modified TiO_2 NTs, which implied fastest decomposition rate and highest gas phase PC activity. The enhanced PC activity can be ascribed the formation of Schottky-junction between NMNs and TiO_2 NTs.
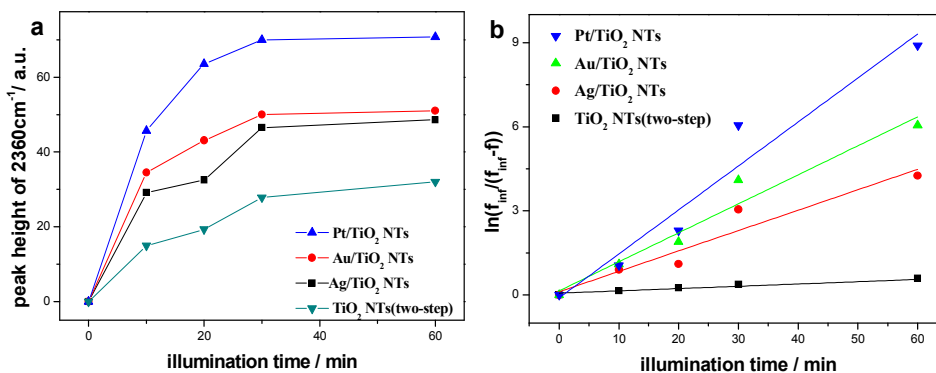
Fig. 6. (a) Variation of the peak height of 2360 cm^{-1} corresponding to the normal vibration of CO_2 molecules derived from the FTIR transmittance spectra with the irradiation time; (b) comparation performance of constant k on TiO_2 NTs and NMNs/TiO_2 NTs respectively.

On the basis of the experimental results, the mechanism of gas phase PC methanol was also discussed here. As illuminated with energy higher than the band gap of TiO_2, electrons (e$^-$) on valence band will be excited to the conduction band, at the same time in the valence band a positively charged hole (h$^+$) is produced, those

electron-holes generated after excitation move quickly to surface from inside and the electrons will transfer to NMNs through the Schottky interface of TiO_2 and NMNs. Under the condition of PC oxidation on methanol, the oxygen adsorbing on the surface of the catalyst was reduced to $\cdot O_2^-$ by photoelectrons on TiO_2 and NMNs surface, and trace water is oxidized to $\cdot OH$ by such holes, which both provide highly active oxidant for the methanol oxidation. The $\cdot O_2^-$ and $\cdot OH$ radicals attack C-H bond in methanol, and then with lively hydrogen atoms to form new free radicals, which stimulates chain reaction, and first oxidation is to form aldehyde then to formic acid, and then ultimately make methanol deeply decompose to H_2O and CO_2. The reaction process is shown in Scheme 3.
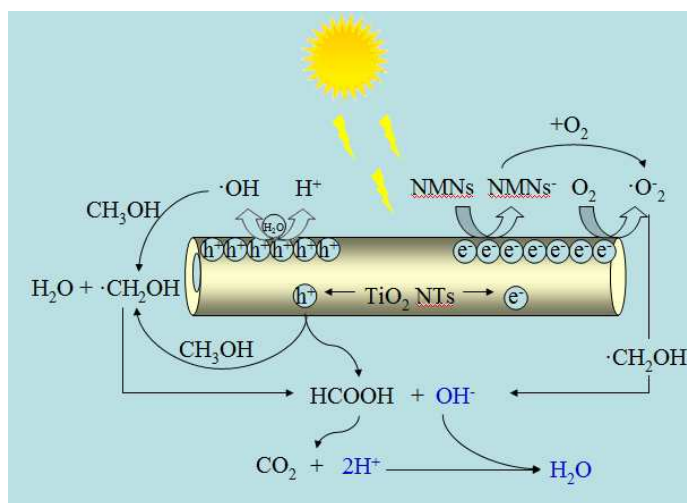
Scheme 3. Photocatalytic mechanism of NMNs/TiO_2 NTs

Conclusions

In summary, noble metal nanoparticles decorated hierarchical TiO_2 NTs were successfully designed with a photocatalytic reduction method and tested the PC activity of degradation of gaseous methanol. It can know that the Pt/TiO_2 NTs afforded the best degradation effect of methanol into CO_2 and have the biggest degradation rate in all three kinds of NMNs/TiO_2 NTs. It had been revealed that noble metal modified the inherent properties of TiO_2 NTs as well as affected the PC activity. The NMNs/TiO_2 NTs meaningfully proved the electron transfer and reduced the recombination of photoelectrons and holes. Compared with the pure TiO_2 NTs, the Pt/TiO_2 NTs showed an outstanding enhancement on PC decomposition of methanol.

Acknowledgements

Notes and references

1 Chen X., Mao S. S. Chem. Rev., 2007, **107**, 2891.

2 Kubacka A., Fernandez-Garcia M. and Colon G., Chem. Rev.,2012, **112**, 1555.

3 J. H. Pan, Z.Lei, W. I. Lee, Z. Xiong, Q. Wang and X. S. Zhao, Catal. Sci. Technol.,2012, **2**, 147.

4 Zhang J., Chen W., Xi J. and Ji Z.， Mater. Lett., 2012, **79**, 259.

5 Wang Y., Feng C., Jin Z., Zhang J., Yang J. and Zhang S., J Mol Catal A: Chem., 2006, **260**, 1.

6 Y. Wang, K. Yu, H. H. Yin, C. Q. Song, Z. L. Zhang, S. C. Li, H. Shi, Q. F. Zhang, B. Zhao, Y. F. Zhang and Z. Q. Zhu, J. Phys. D: Appl. Phys., 2013, **46**, 175303.

7 Wu H. and Zhang Z., Int J. Hydrogen Energy, 2011,**36**, 13481.

8 Wu H. and Zhang Z., J. Solid State Chem., 2011, **184**, 3202.

9 Mor G. K., Shankar K. and Paulose M., Varghese O. K. and Grimes C. A., Nano Lett., 2006, **6**, 215.

10 Zhang Z. and Wang P., Energy Environ. Sci., 2012, **5**, 6506.

11 Tauster, S. J., Fung, S. C., Garten and R. L. J. Am. Chem. Soc., 1978, **100**, 170.

12 V Iliev, D Tomova, L Bilyarska, A Eliyas and L Petrov, Catal. Commun., 2004, **5**, 759.

13 Seery, M. K., George, R., Floris, P., Pillai and S. C. J. Photoch. Photobio.A. Chem., 2007, **189**, 258.

14 Z. W. Seh, S. Liu, S. Y. Zhang, K. W. Shah and M. Y. Han. Chem. Commun. 2011, **47**, 6689.

15 Z. W. Seh, S. Liu, S. Y. Zhang, M. S. Bharathi, H. Ramanarayan , M. Low, K. W. Shah, Y. W. Zhang and M. Y. Han, Angew. Chem. Int. Ed. 2011, **50**, 10140.

16 Z. W. Seh, S. Liu, M. Low, S. Y. Zhang, Z. Liu, A. Mlayah and M. Y. Han, Adv. Mater. 2012, **24**, 2310.

17 A. A. Ismail and D. W. Bahnemann, J. Phys. Chem. C, 2001, **115**, 5784.

18 Z. Zheng, B. Huang, X. Qin, X. Zhang, Y. Dai and M. H. Whangbo, J. Mater. Chem., 2011, **21**, 9079.

19 X.J. Feng, J. D. Sloppy, T. J. LaTemp, M. Paulose, S. Komarneni, N. Z. Bao and C. A. Grimes, J. Mater. Chem., 2011, **21**, 13429.

20 Y. Zhang, W. Rong, Y. Fu, X. Ma and J. Polym. Environ., 2011, **19**, 966.

21 M. Mohseni and A. Dvaid. Appl. Catal. B-Environ., 2003, **46**, 219.

22 N. Djeghri, M. Formenti and F. Juillet. Faraday. Discuss. Chem. Soc., 1974, **60**, 369.

23 W. Choi, JY Ko, H Park and J.S. Chung, Appl. Catal. B-Environ., 2001, **31**, 209.

24 Akawat Sirisuk , Charles G. Hill and Marc A. Anderson, Catal. Today, 1999, **54**, 159.

25 H. Wu, Y. Wang, Y. Ma, T. Xiao, D. Yuan and Z. Zhang. Ceramics International, 2015, **41**, 2527.

26 Z. Zhang, L. Zhang, M. N. Hedhili, H. Zhang, and P. Wang. Nano Lett. 2013, **13**, 14.

27 D. Yuan,Y. Gao, H. Wu,,T. Xiao,Y. Wang, B. Wang and Z. Zhang, RSC Adv., 2014, **4**, 19533

28 C. Binet and M. Daturi, Catal. Today, 2001, **70**, 155.

29 Z. Zhang, M. F. Hossain, T. Arakawa and T. Takahashi, J. Hazard, Mater., 2010, **176**, 973.

30 K. Prabakar,T. Takahashi, T. Nakashima, Y. Kubota and A. Fujishima, J. Vac. Sci. Technol. A, 2006, **24**, 1613.

31 K. Mudalige, S. Warren and M. Trenary, J. Phys. Chem. B, 2000, **104**, 2448.

32 Colley C. S., Kazarian S. G., Weinberg P. D. and Lever M. J., Biopolymers, 2004, **74**, 328.

33 G. Kister, G. Cassanas and M. Vert, Polymer, 1998, **39**, 267.

34 F. Ouyang, S. Yao, K. Tabata and E. Suzuki, Appl. Surf. Sci., 2000, **158**, 28.

35 A. L.Goodman, L. M. Campus and K. T. Schroeder, Energy Fuels, 2005, **19**, 471.

36 Zhang Z., Hossain M. F., Miyazaki T. and Takahashi T., Environ Sci Technol., 2010, **44**, 4741.